


Cite this: *RSC Adv.*, 2024, 14, 24815

Fabrication and biocompatibility evaluation of hydroxyapatite–polycaprolactone–gelatin composite nanofibers as a bone scaffold

Aminatun,^a Aisyah Sujak M. K.,^a Djony Izak R.,^a Sofijan Hadi,^b Yessie Widia Sari,^c Gunawarman,^d Nilam Cahyati,^e Yusril Yusuf^e and Che Azurahaman Che Abdullah^f

One approach to addressing bone defects involves the field of bone tissue engineering, with scaffolds playing an important role. The properties of the scaffold must be similar to those of natural bone, including pore size, porosity, interconnectivity, mechanical attributes, degradation rate, non-toxicity, non-immunogenicity, and biocompatibility. The primary goals of this study are as follows: first, to evaluate hydroxyapatite (HA)/polycaprolactone (PCL)/gelatin nanofiber scaffolds based on functional groups, fibre diameter, porosity, and degradation rate; second, to investigate the interaction between HA/PCL/gelatin scaffolds and osteoblast cells (specifically, the ATCC 7F2 cell line) using *in vitro* assays, including cell viability and adhesion levels. The fibre samples were fabricated using an electrospinning technique with a 15 kV voltage, a spinneret-collector distance of 10 cm, and a flow rate of 0.3 mL hour⁻¹. The process was applied to five different HA/PCL/gelatin concentration ratios: 50 : 40 : 10; 50 : 30 : 20; 50 : 25 : 25; 50 : 20 : 30; 50 : 35 : 15 (in %wt). Fourier Transform Infrared (FTIR) spectrum analysis and tests revealed no differences in functional groups across the five compositions. The identified functional groups include PO₄³⁻, OH⁻, CO₃²⁻ and C=O stretching. Notably, an increase in PCL concentrations resulted in larger fiber diameters, ranging from 369–1403 nm with an average value of 929 ± 175 nm. The highest porosity percentage was (77.27 ± 11.57) %, and a sufficient degradation rate of up to 3.5 months facilitated the proliferation process of osteoblast cells. Tensile strength assessments revealed a significant increase in tensile strength with the addition of PCL, reaching a peak of 1.93 MPa. The MTT assay demonstrated a discernible increase in cell proliferation, as evidenced by increased cell viability percentages on days 1, 3, and 5. Concurrently, the fluorescence microscopy examination indicated an increase in cell numbers, which was especially noticeable on days 1 and 5. The SEM analysis confirmed the biocompatibility of the HA/PCL/gelatin nanofiber scaffold, as osteoblast cells attached and dispersed successfully five days after seeding. Based on these findings, the HA/PCL/gelatin nanofiber scaffold emerges as a very promising candidate for treating bone damage.

Received 2nd April 2024

Accepted 17th July 2024

DOI: 10.1039/d4ra02485k

rsc.li/rsc-advances

Introduction

The use of scaffolds has become a solution, for addressing bone damage or degeneration playing a role in restoring and regenerating tissue functionality. These scaffolds act as structures supporting cell growth and the deposition of the matrix until the complete restoration of the matrix is achieved.¹ The ideal

characteristics of a scaffold include being highly compatible with living tissues having a good ratio of surface area to volume, significant porosity and interconnected pores^{2,3} as being mechanically stable and biologically functional at the site where it is implanted.⁴

Nanofibers have garnered attention as candidates for bone scaffolds due to their customizable properties that enable them to mimic the structure of the extracellular matrix (ECM). The ability to adjust the diameter and porosity of nanofibers during fabrication allows for cell adhesion and interaction with ECM components. Additionally these nanofibers offer a surface area to their volume, which promotes efficient adsorption and widespread cell immobilization.⁵

Currently there are methods for fabricating nanofibers with electrospinning standing out as a prominent technique. Electrospinning is used to create fibers with diameters greater than one micron and high levels of porosity. Scaffolds produced

^aDepartment of Physics, Universitas Airlangga, Surabaya 60115, Indonesia. E-mail: aminatun@fst.unair.ac.id

^bDepartment of Chemistry, Universitas Airlangga, Surabaya 60115, Indonesia

^cDepartement Physics, Institut Pertanian Bogor, Bogor 16680, Indonesia

^dDepartment of Mechanical Engineering, Universitas Andalas, Padang 25163, Indonesia

^eDepartement of Physics, Universitas Gadjah Mada, Yogyakarta 55281, Indonesia

^fInstitute of Nanoscience and Nanotechnology, Universiti Putra Malaysia, UPM Serdang, 43400, Selangor, Malaysia



using this method have shown potential, in creating an environment that supports bone formation. In addition electrospinning enables the creation of nanofibers using types of polymers including those that can naturally break down and are compatible, with living organisms. It also allows for the production of compounds made from materials.⁶

Choosing the biomaterials is crucial when it comes to forming bone tissue. Scaffolds designed for bone regeneration should possess properties that promote bone formation support the growth of bone and surrounding tissues integrate seamlessly with existing bone structures and be both biologically friendly and capable of breaking down over time. These scaffolds should also have a structure to bone.² Recent advancements in scaffold technology in nanofiber fabrication techniques like electrospinning have demonstrated potential in creating scaffolds that create an environment for efficient bone repair. These developments highlight the need for research and innovation, in scaffold development to enhance bone healing and regeneration.

The primary inorganic constituent of bone tissue, hydroxyapatite (HA), is commonly used in bone scaffolds. The chemical structure of HA, which closely resembles the minerals found in human bone tissue, allows for a high chemical affinity for bonding with bone. Although HA has a Young's modulus ranging from 35 to 120 GPa, its inherent brittleness necessitates the incorporation of polymers to improve its mechanical properties.⁷ Polycaprolactone (PCL) has been widely used in biomaterials since the 1970s and 1980s. Despite receiving little attention for several decades, PCL has recently seen a surge in applications, most notably in the expanding field of tissue engineering. PCL is known for its favourable mechanical properties, ease of fabrication, and cost-effectiveness when compared to other polymers. It is also known for its biodegradability, bioresorbability, and biocompatibility with the body.⁸ Scaffolds made of polycaprolactone (PCL) provide long-term support in the field of soft tissue engineering, effectively promoting the growth of adjacent tissue, with PCL having a two-year degradation period.⁹ PCL has a wide range of applications, including connective tissue repair and regeneration.¹⁰ The incorporation of natural polymers, such as gelatin, improves the interaction of hydroxyapatite (HA)-PCL scaffolds with cells. Gelatin, due to its biocompatibility, biodegradability, and low antigenicity, can be synergistically combined with other inorganic supporting materials to improve each constituent's mechanical properties and cell interaction.^{11,12} Because of its similarity to the natural extracellular matrix (ECM) of bone, the combination of gelatin and HA is promising for long-term applications.² Gelatin, when combined with PCL, produces bone scaffolds with a tensile strength of 3.7 MPa.¹³ Therefore, scaffolds which are only made of polymers, are not ideal in terms of mechanical strength. Thus, the combination of polymers with active bioceramics such as HA is the right choice to maintain the biological and mechanical balance.¹⁴

Given the context, the goal of this article is to investigate the properties of bone scaffolds made from the HA/PCL/gelatin composite. Based on several previous studies, the mechanical properties of nanofibers using PCL are influenced by several factors such as the size of the fiber diameter, orientation, and

overall structure.^{15,16} Then, a nanofiber study of a three-material composite such as HEC/PVA/collagen showed a significant decrease in Young's modulus and tensile stress over 12 weeks, thus meeting the requirements of the potential of biodegradable biomaterials for skin replacement.¹⁷ This shows that degradation is also an important factor in nanofiber scaffolds. Therefore, in this study, the initial investigation focus on assessing HA/PCL/gelatin scaffolds in terms of their physicochemical properties, which include functional group analysis and scaffold morphology parameters such as fibre diameter size, mechanical properties, porosity, and degradation. Following that, the secondary focus involves examining the interaction between HA/PCL/gelatin scaffolds and osteoblast cells using an *in vitro* assay that includes cell viability and adhesion levels.

Material and methods

The materials used in this study include polycaprolactone (PCL) with a molecular weight of 80 000 from Sigma-Aldrich, hydroxyapatite, chloroform, 96% ethanol solution, distilled water, acetone, 1% sodium hydroxide (NaOH), and extra pure gelatin (SAP-G 003) procured from UD Sumber Ilmiah Persada, Surabaya, Indonesia. Additionally, osteoblast cell culture ATCC 7F2, DMEM, trypsin, Phosphate Buffer Saline (PBS), mixed medium (DMEM + 10% FBS + 1% amphotericin + penicillin sertraline), a graded alcohol series (50%, 60%, 70%, 80%, 90%, 100%), dimethyl sulfoxide (DMSO), propidium iodide solution (PI), 4',6-diamidino-2-phenylindole (DAPI), and 2.5% glutaraldehyde solution were employed.

Research procedures

There were two phases to the research process. Stage (A) involved the electrospinning technique to create HA/PCL/gelatin nanofiber scaffolds, followed by their physicochemical characterization. The *in vitro* experiment that characterised the scaffold–osteoblast cell interaction was the main focus of stage (B). The research process is described in detail in Fig. 1.

Fabrication of HA/PCL/gelatin nanofiber scaffolds

The HA/PCL/gelatin compositions indicated as (A) 50 : 40 : 10, (B) 50 : 30 : 20, (C) 50 : 25 : 25, (D) 50 : 20 : 30, and (E) 50 : 35 : 15 in weight percent (wt%) were used to create the scaffolds. At first, separate solutions were made for every component. For example, sample A's 0.5 g of HA powder, 4 g of PCL, and 0.1 g of gelatin powder were dissolved in 1 mL of distilled water, 10 mL of chloroform, and 1 mL of distilled water, respectively. Following their individual preset weight ratios, samples B, C, D, and E underwent the same preparation procedure twice. The sample A solution was then formed by combining the component solutions and homogenising them for three hours at room temperature with a magnetic stirrer. The electrospinning process was then used to create nanofibers. The sample A solution was loaded into a 10 mL syringe fitted with a 21-gauge × 1.5-inch blunt-tip needle and connected to a high-voltage power supply. The electrospinning parameters used in this study were a 15 cm distance



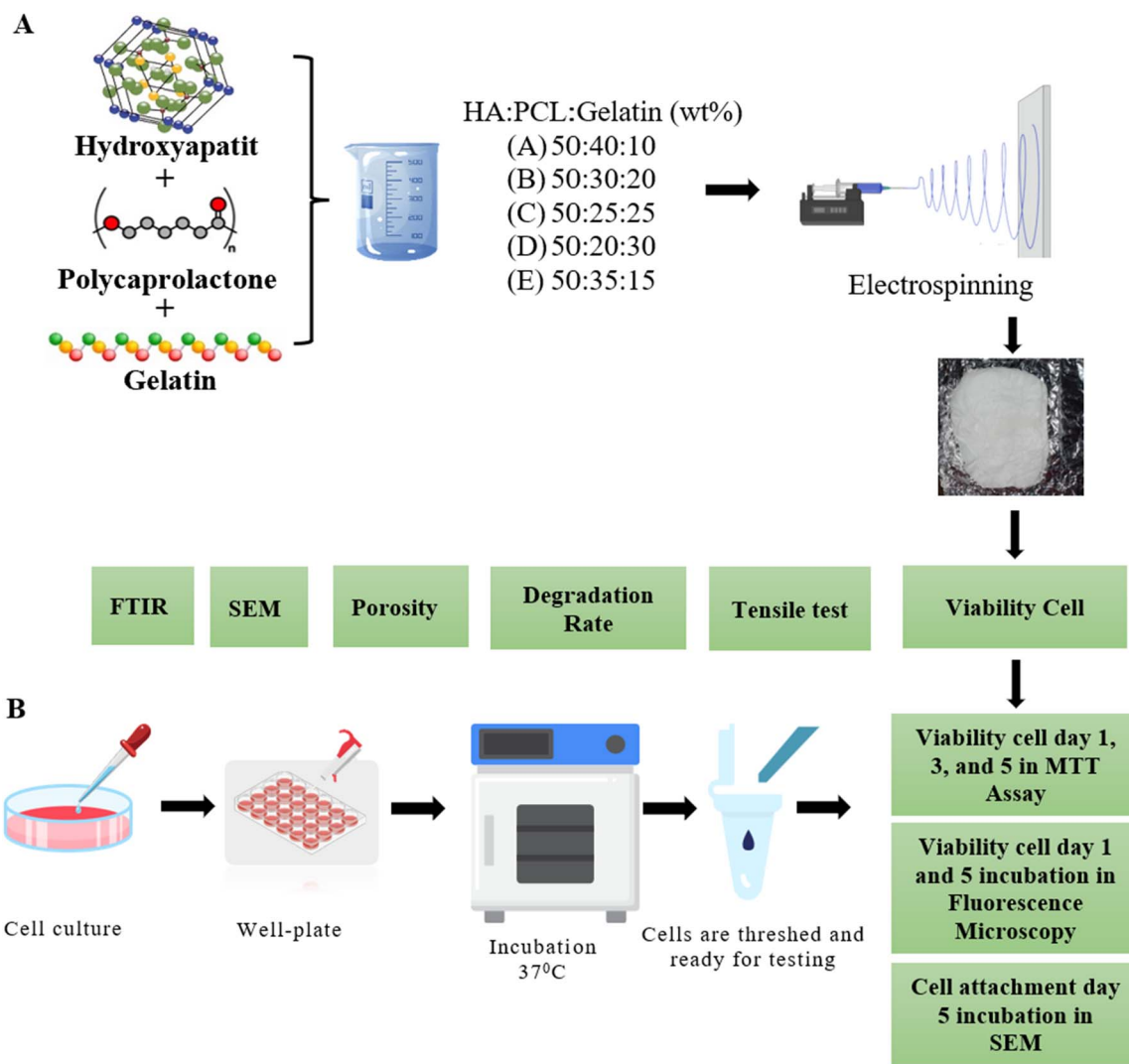


Fig. 1 HA/PCL/gelatin nanofiber fabrication procedure and characterization: (A) psycho-chemical characterization and (B) characterization by *in vitro* assay of scaffold interactions with osteoblast cells.

between the needle and collector, a voltage of 23 kV, and a flow rate of 0.3 mL h⁻¹. This electrospinning process was repeated until the solution was depleted, which took approximately 3.5 hours. The resulting nanofibers were then allowed to settle at room temperature before being further characterised.

Characterization

Functional group test using fourier transform infrared (FTIR) spectrophotometer

The functional groups of the HA/PCL/gelatin nanofiber were analyzed using an FTIR (Shimadzu IRTracer-100) in the wave-number range of 500–4000 cm⁻¹.

HA/PCL/gelatin nanofiber scaffold diameter measurement *via* scanning electron microscope (SEM)

A Hitachi TM3000 Tabletop Microscope with a magnification of 10 000× was used to characterise the morphology of the HA/PCL/gelatin nanofiber scaffold. The fibre diameters were

determined by analysing SEM observation images with the ImageJ application. The image's pixel size was first calibrated against a reference size, which is typically displayed on SEM images as a line with a scale indicating the level of magnification. The diameters of 100 fibres were measured at random and the results were displayed in a histogram.

Porosity test of HA/PCL/gelatin nanofiber scaffold

Porosity, defined as the ratio of the volume of pores in a material to its overall volume, was assessed to determine the extent of porosity formed, with ideal porosity for bone growth being between 70–90%. The liquid displacement method was employed for this test. Initially, the sample volume (*v*) and dry mass (*W_d*) were measured. The samples were then immersed in a 96% ethanol solution for 48 hours. Post-immersion, the sample wet mass (*W_w*) was measured.

$$\text{Porosity} = \frac{W_w - W_d}{W_w} \times 100\% \quad (1)$$



Degradation rate measurement of HA/PCL/gelatin nanofiber scaffold

Degradation testing determined the longevity of the samples in the body after implantation. Phosphate-buffered saline (PBS) was used as the buffer solution. The sample mass before immersion in PBS was recorded as W_0 . The sample was then immersed in PBS for periods of 7, 14, 21, and 28 days, with its mass measured again as W_1 . The percentage of mass loss was calculated using eqn (2).

$$\text{Mass loss(\%)} = \frac{W_0 - W_1}{W_0} \times 100\% \quad (2)$$

The degradation rate was calculated by dividing the mass loss on days 7, 14, 21, and 28 by the immersion time.

Mechanical properties measurement of HA-PCL-gelatin nanofiber scaffold

Tensile strength testing was carried out on the sample to determine its durability against tensile loads using the Shimadzu Universal Testing Machine AGS 1kNX. The samples were formed into a dog bone shape using the American Standard Testing and Material (ASTM) type V. The specimen was attached to the tensile testing apparatus on both ends and subjected to opposing tensile forces until rupture occurred. Following the test, various mechanical properties such as Ultimate Tensile Strength (UTS), Elastic modulus (E), and elongation were calculated using eqn (3)–(5) respectively.

$$\text{Ultimate tensile strength} = \sigma = \frac{F}{A} \text{ (MPa)} \quad (3)$$

$$\text{Elastic modulus} = E = \frac{\sigma}{\epsilon} \text{ (MPa)} \quad (4)$$

$$\text{Elongation} = \frac{nL}{L} \times 100\% \quad (5)$$

where σ = stress (N m^{-2}), F = load (N), A = cross-sectional area (m^2), ϵ = strain = $\frac{\Delta L}{L}$, L = initial sample length (m), and ΔL = the difference in length after stretching.

Cytotoxicity test MTT assay scaffold nanofiber HA/PCL/gelatin

The cytotoxicity assessment is a method to assess a material's direct toxic impact on cell cultures. The procedure began with the culture of osteoblast cells (ATCC 7F2) in a 75 cm^2 flask in Dulbecco's Modified Eagle Medium (DMEM) at 37 °C with 5% CO_2 in the air. The culture medium was changed every 48–72 hours until a single confluent layer established. A trypsin–ethylene diamine tetraacetic acid (EDTA) solution in Phosphate Buffered Saline (PBS) was used to harvest the cells. The flask was then filled with 1–2 mL of trypsin–EDTA solution and placed in a 37 °C incubator until cell detachment occurred. The HA/PCL/gelatin scaffold samples were cleaned with PBS to neutralise the pH before being cut into 0.3 $\text{cm} \times 0.3 \text{ cm}$ pieces. These samples were sterilised by exposing them to ultraviolet light for 15 minutes. Following that, cultured osteoblast cells were placed in 96-well and 48-well plates,

with 100 μL of medium containing 3000 cells per well and 200 μL of medium containing 5000 cells per well, respectively. The samples were cut and sterilised before being placed in well plates filled with cell-containing medium and incubated at 37 °C for 1 day in the 96-well plates and 3 and 5 days in the 48-well plates, with regular monitoring and medium replacement. The medium was checked and replaced during the incubation period. Following that, 20 μL of MTT dissolved in PBS was added to each well and incubated at 37 °C for 4 hours. The HA/PCL/gelatin nanofiber scaffold samples were removed from the wells after incubation, and 10 μL of MTT solution (3-(4,5-dimethyl-2-thiazolyl)-2,5-diphenyl-2H-tetrazolium bromide) was added to each well. The MTT solution was then discarded, and 100 μL of dimethylsulfoxide (DMSO) solubilization solution was added to each well in the 96 well-plate and 200 μL in the 48 well-plates to dissolve the formazan crystals or stop the MTT reaction. An Epoch Microplate Spectrophotometer was used to read each well at a wavelength of 570 nm.

$$\text{Cell viability} = \frac{\text{OD treatment} - \text{OD media control}}{\text{OD cell control} - \text{OD media control}} \times 100\% \quad (6)$$

Fluorescence microscopy test

This test was performed to observe live and dead osteoblast cells interacting with the HA/PCL/gelatin nanofiber scaffold. The osteoblast cells were placed in a 42-well plate and incubated for 24 hours in a mixed medium (DMEM + 10% FBS + 1% amphotericin). After discarding the medium, 100 μL of new mixed DMEM medium was added. The samples were then replaced in the 42-well plate. The samples and medium were incubated for 24 and 120 hours at 37 °C. PBS was used to fix the attached cells, followed by trypsin treatment and centrifugation. The dilution of DAPI and PI was performed by diluting 10 μL of DAPI/PI in 2 mL of distilled water, then taking 2.1 μL and mixing it with 100 μL of PBS. Following this, 1 μL was taken and diluted in 1000 μL of PBS. The microscope slide object glass was then covered with a cover glass and placed on the fluorescence microscope stage for observation at 10 \times magnification. Living cells were displayed in blue and dead cells in red.

Attachment cell test with SEM (scanning electron microscopy)

In a 48-well plate, HA/PCL/gelatin nanofiber scaffold samples were incorporated with osteoblast cells in a mixed medium (DMEM + 10% FBS + 1% amphotericin + penicillin sertraline), then incubated at 37 °C for 5 days. After 5 days, the samples were taken out of the incubator, rinsed twice with PBS, and fixed for 2 hours in a 2.5% glutaraldehyde solution. This was followed by dehydration with ethanol at increasing concentrations (50%, 60%, 70%, 80%, 90%, and 100%, v/v). The samples were dried at room temperature before they were coated with gold for 60 seconds using a sputter coater. Finally, a scanning electron microscope (SEM) was used to examine the samples.

Data analysis

The data obtained from the fluorescence microscopy and SEM tests were subjected to qualitative analysis, while the MTT Assay



data were processed quantitatively using the Statistical Package for the Social Sciences (SPSS). The initial step involved descriptive analysis, focusing on the calculation of mean values and standard deviation for each variable. Subsequently, to evaluate the normal distribution of the data, normality tests, specifically the Kolmogorov–Smirnov and Shapiro–Wilk tests, were employed, accompanied by the homogeneity test (Levene's test). Should the data display normal distribution and homogeneity, a One-way ANOVA test was then executed to determine the statistical significance of the findings. In instances of significant differences, a Post Hoc Tukey HSD test was applied to further examine the differences across various treatments.



Fig. 2 Fabrication results of HA/PCL/gelatin nanofiber scaffolds.

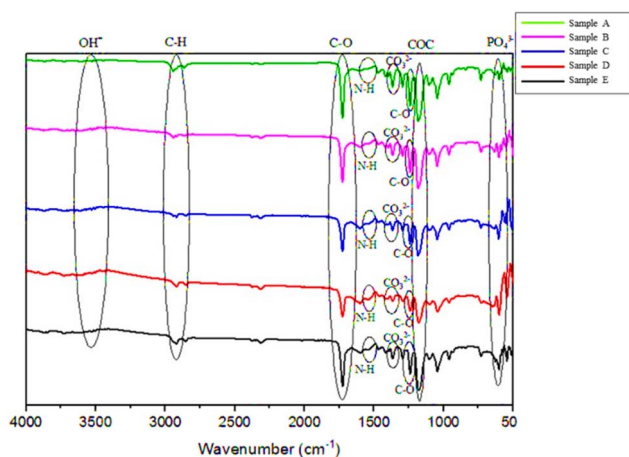


Fig. 3 FTIR spectrum of HA/PCL/gelatin with varying ratios of sample (A) (50 : 40 : 10), sample (B) (50 : 30 : 20), sample (C) (50 : 25 : 25), sample (D) (50 : 20 : 30), and sample (E) (50 : 35 : 15).

Results and discussion

Electrospinning was used to successfully fabricate nanofiber scaffolds made of HA/PCL/gelatin using five different weight ratios of HA, PCL, and gelatin, designated as A (50 : 40 : 10), B (50 : 30 : 20), C (50 : 25 : 25), D (50 : 20 : 30), and E (50 : 10 : 40). Fig. 2 depicts a representative sample of these nanofibers.

Functional group analysis of FTIR spectrum

FTIR testing was employed to identify the functional groups within compound bond vibrations. The current study characterized five samples with FTIR testing, specifically HA/PCL/gelatin samples, each exhibiting different concentration ratios. The spectrum analysis results of the HA/PCL/gelatin scaffold are presented in Fig. 3.

The FTIR characterization indicated the presence of hydroxyapatite functional groups such as PO_4^{3-} , OH^- , and CO_3^{2-} . The CO_3^{2-} group emerged due to the reaction between HA and CO_2 in the atmosphere during the fabrication process. This presence of CO_3^{2-} is not considered detrimental, given that human bones naturally contain CO_3^{2-} , which substitutes for PO_4^{3-} in the formula $\text{Ca}_{10}(\text{CO}_3)_x(\text{PO}_4)_{6-(2/3)x}(\text{OH})_2$, commonly referred to as carbonated-hydroxyapatite.^{18–20} In PCL, several groups were detected, including asymmetric stretching vibrations in CH_2 at the wavenumber 2941.44 cm^{-1} and $\text{C}=\text{O}$ stretching at 1600.92 cm^{-1} . Stretching vibrations in the crystalline phase of $\text{C}-\text{O}$ and $\text{C}-\text{C}$ appeared at wavenumbers 1294.24 and 1292.31 cm^{-1} , respectively. Asymmetric COC stretching vibrations were observed at 1240.23 ; 1238.30 ; 1240.23 cm^{-1} .²¹ Functional groups of gelatin compound were found at absorption wavenumbers 1598.99 and 1544.98 cm^{-1} ($\text{N}-\text{H}$ stretching from secondary amides), and $\text{C}-\text{H}$ stretching at around 2864.29 cm^{-1} . These findings suggest that the HA/PCL/gelatin nanofiber samples did not exhibit any chemical interaction, as no differences in functional groups were observed among the five HA/PCL/gelatin samples.

SEM test result

The surface morphology of the HA/PCL/gelatin scaffold was characterized using a Scanning Electron Microscope (SEM). The result of the SEM test at $10\,000\times$ magnification can be seen in Fig. 4 (left), which displays the scaffold surface, and Fig. 4 (right), which illustrates the distribution of fiber diameters.

Fig. 4 demonstrates that fibers were perfectly formed in all five samples, each exhibiting varying fiber diameters, as measured using the ImageJ application. The distribution of these diameters is detailed in Table 1.

Table 1 Fiber diameter

Sample	HA : PCL : gelatin (wt%)	Fiber diameter (nm)	Average fiber diameter (nm)
A	50 : 40 : 10	369–1403	929 ± 175
B	50 : 30 : 20	234–1650	797 ± 122
C	50 : 25 : 25	204–1281	495 ± 117
D	50 : 20 : 30	233–1174	492 ± 102
E	50 : 35 : 15	388–2676	1406 ± 193

Porosity test results

Porosity, defined as the percentage of void space within a solid, was calculated as per eqn (1), with the results presented in Fig. 5. Fig. 5 shows that the porosity percentage in scaffold samples with compositions of 50 : 40 : 10, 50 : 30 : 20, 50 : 25 : 25,

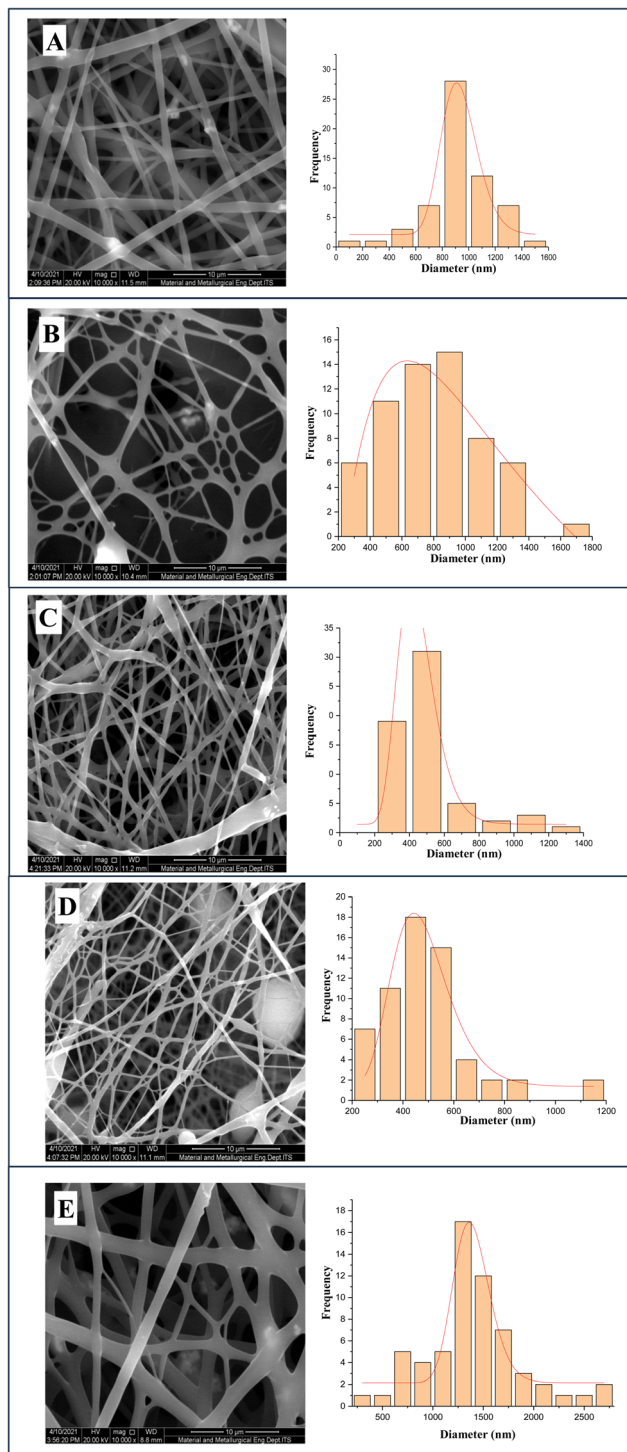


Fig. 4 SEM test results – 10 000 \times magnification and distribution of fiber diameters for HA/PCL/gelatin samples with variations in the ratio of sample (A) 50 : 40 : 10 sample (B) 50 : 30 : 20 sample (C) 50 : 25 : 25 sample (D) 50 : 20 : 30 and sample (E) 50 : 35 : 15.

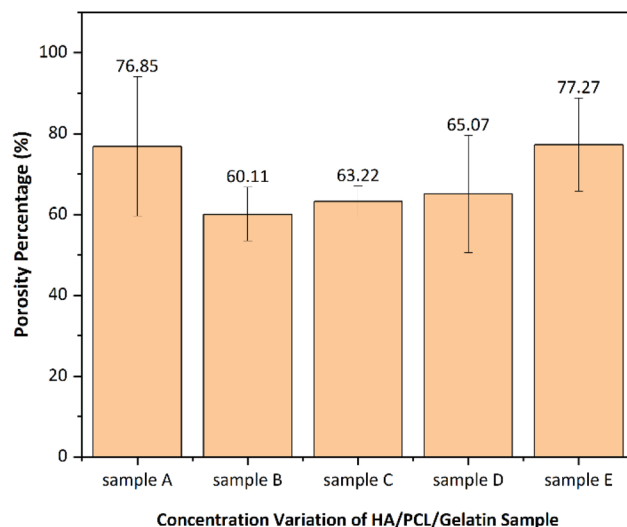


Fig. 5 Graph of porosity test results for HA/PCL/gelatin nanofiber scaffold samples (in wt%): (A) 50 : 40 : 10, (B) 50 : 30 : 20, (C) 50 : 25 : 25, (D) 50 : 20 : 30 and (E) 50 : 35 : 15.

50 : 20 : 30, and 50 : 35 : 15 decreased as the concentration of PCL decreased and increased with the addition of gelatin.

The increased porosity is significant because it allows bone tissue cells to infiltrate and multiply within the scaffold pores, increasing osteoconductivity.²² An ideal scaffold design strives to mimic the morphology, structure, and functionality of natural bone, allowing for seamless integration into the surrounding tissue. Human cancellous bone has an extensive network of trabeculae and a porosity value ranging from 50–90%.²³

The results of the tests revealed that all variations of the samples had porosity percentages within the typical range associated with cancellous bone.

Degradation test result

Degradation testing was pivotal in determining the degradation rate of the HA/PCL/gelatin scaffold samples in Stimulated Body Fluid (SBF). Sample degradation occurred up to the third week, totaling 21 days, a period during which new apatite particles formed, potentially decomposing the apatite crystals in fractured bone tissue. Notably, physical changes were observed, characterized by the gradual disintegration of the sample due to the impact of the Stimulated Body Fluid (SBF) environment.²³ The degradation rate was calculated based on the percentage of mass loss, as outlined in eqn (2). Fig. 6 presents the results, detailing the percentage of mass loss (% mass loss) of the HA/PCL/gelatin nanofiber samples.

A porous scaffold with a suitable degradation percentage should be used for bone regeneration. The degradation of biomaterials is critical in the replacement of the material with newly formed bone, and the degradation timeline should coincide with the bone healing process.²⁴ Fig. 6 shows the predicted degradation rate and time frame for complete degradation of the samples. Table 2 contains all of this information.

An essential component of tissue engineering is degradation. Scaffold degradation must not occur too quickly so that



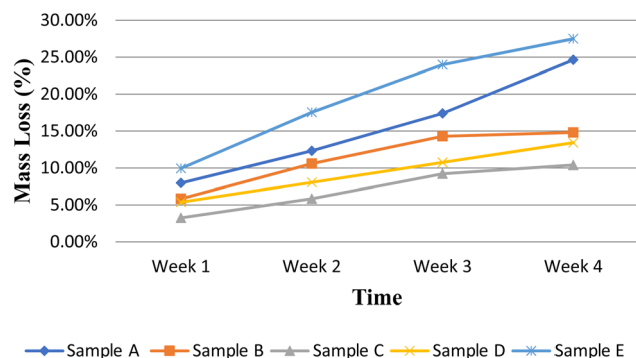


Fig. 6 Degraded mass percentage of HA/PCL/gelatin nanofiber scaffold samples (in wt%): (A) 50 : 40 : 10, (B) 50 : 30 : 20, (C) 50 : 25 : 25, (D) 50 : 20 : 30 and (E) 50 : 35 : 15.

Table 2 Estimated degradation rate and total degraded time

Sample	HA : PCL : gelatin (wt%)	Degradation rate (g h^{-1})	Degraded time (month)
A	50 : 40 : 10	1×10^{-4}	0.38
B	50 : 30 : 20	1×10^{-4}	0.26
C	50 : 25 : 25	6×10^{-5}	3.51
D	50 : 20 : 30	7×10^{-5}	2.91
E	50 : 35 : 15	1×10^{-4}	0.23

cells have enough time to multiply. Degradation, however, has the potential to interfere with the tissue's biological function if it proceeds more slowly than tissue regeneration.²⁵ When scaffold residues are present after tissue regeneration has taken place, neutrophils and macrophages will phagocytose the scaffold remnants. Therefore, a foreign body reaction could be triggered by slow degradation, which could result in severe and unwanted reactions.

Mechanical property test result

The mechanical strength of a scaffold is a crucial parameter. The mechanical strength of the HA/PCL/gelatin scaffold samples was assessed *via* a tensile strength test. The results of this test are compiled in Table 3.

The HA/PCL/gelatin nanofiber sample with a 50 : 40 : 10 ratio (sample A) demonstrated the highest ultimate tensile strength (UTS) value of 1.93 MPa. Meanwhile, in the sample with a 50 : 25 : 25 ratio exhibited the lowest UTS value of 1.02 MPa. Table 3 shows the relationship between the HA/PCL/gelatin variations, tensile strength, modulus of elasticity, as depicted in Fig. 7.

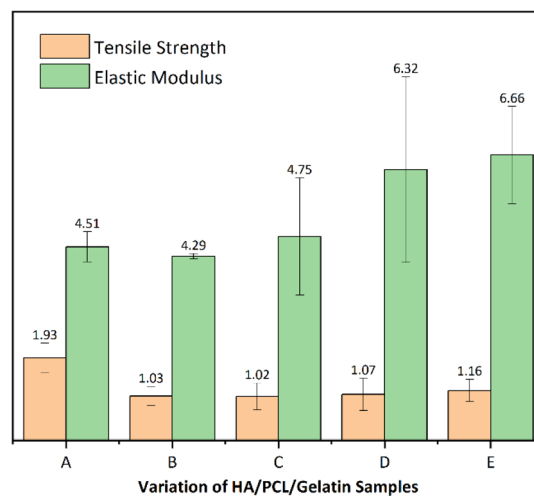


Fig. 7 Ultimate Tensile Strength (UTS) and elastic modulus of HA/PCL/gelatin nanofiber scaffold samples: (A) 50 : 40 : 10, (B) 50 : 30 : 20, (C) 50 : 25 : 25, (D) 50 : 20 : 30 and (E) 50 : 35 : 15 (in wt%).

Fig. 7 depicts a decrease in tensile strength values from A to E, ranging from 1.93 to 1.16 MPa. These values are less than the tensile strength of cancellous bone, which is approximately 7.4 MPa. Notably, a decrease in PCL concentration correlates with a decrease in tensile strength of the scaffold. PCL, a semi-crystalline polymer with excellent mechanical properties, contrasts with gelatin, a natural polymer known for its low mechanical strength.

The HA/PCL/gelatin sample with the highest PCL content, specifically at a ratio of 50 : 40 : 10, had the highest Ultimate Tensile Strength (UTS) value, approximately 1.9 MPa. However, this UTS value remains lower than that of PCL/gelatin, which is 3.7 MPa.¹³ Despite being remarkable, this UTS is not high enough for the application of bone tissue engineering because of its small magnitude in comparison to the UTS of human bone.

MTT assay test result

A cell proliferation evaluation was performed to determine the scaffold's ability to support osteoblast cells for 1, 3, and 5 days. Eqn (6) was used to calculate cell viability. According to the MTT Assay results (Table 4 and Fig. 8), all samples had cell viability greater than 70%. This suggests that the scaffold is non-toxic and promotes cell survival. Furthermore, an increase in cell viability percentages was observed across all samples on days 3 and 5, indicating effective osteoblast cell proliferation, as

Table 3 Mechanical properties of HA/PCL/gelatin nanofiber samples

Sample	HA : PCL : gelatin (wt%)	UTS (MPa)	Modulus of elasticity (MPa)	Elongation (%)
A	50 : 40 : 10	1.93 ± 0.34	4.51 ± 0.35	43.02
B	50 : 30 : 20	1.03 ± 0.23	4.29 ± 0.06	24.0
C	50 : 25 : 25	1.02 ± 0.32	4.76 ± 1.37	21.44
D	50 : 20 : 30	1.07 ± 0.38	6.32 ± 2.03	16.88
E	50 : 35 : 15	1.16 ± 0.26	6.66 ± 1.14	17.35

Table 4 MTT assay test result

Sample	HA : PCL : gelatin (wt%)	Cell viability (%)		
		Day-1	Day-3	Day-5
A	50 : 40 : 10	76.99 ± 5.06	101.56 ± 7.68	102.32 ± 15.56
B	50 : 30 : 20	78.56 ± 4.65	103.11 ± 12.65	105.99 ± 8.94
C	50 : 25 : 25	78.28 ± 3.07	104.10 ± 8.56	102.86 ± 11.86
D	50 : 20 : 30	79.33 ± 11.33	104.88 ± 5.86	103.78 ± 11.88
E	50 : 35 : 15	78.70 ± 10.99	106.92 ± 3.40	108.83 ± 7.38

evidenced by cell viability percentages exceeding 101% for all samples on days 3 and 5.

After the MTT assay results (Table 4), a statistical analysis was conducted using the Statistical Package for the Social Sciences (SPSS), with the findings presented in Table 5. Table 5 infers that while all data vary significantly over time, they do not exhibit significant variation in terms of composition. A *p*-value of <0.05 is indicative of significant differences.

Visualization result of living and dead cells

Fluorescence microscopy was used to observe the interactions of living and dead cells with the HA/PCL/gelatin nanofiber scaffold on days 1 and 5 (Table 6). The results of this assessment are shown in Fig. 9 and Fig. 10, which show living cells and dead cells, respectively. FIJI was used to calculate the number of living and dead cells on days 1 and 5. Living cells emit blue fluorescence, while dead cells emit red fluorescence. The scaffold was mostly occupied by living cells on the first day, with only a few dead cells. By day 5, the cell count had increased, primarily filling the nanofibrous scaffold with blue fluorescence, indicating living cells, and a relatively low level of red fluorescence, indicating dead cells Fig. 11.

Table 5 MTT assay test result

Sample	HA : PCL : gelatin (wt%)	Sig. (p)
A	50 : 40 : 10	0.002
B	50 : 30 : 20	0.019
C	50 : 25 : 25	0.008
D	50 : 20 : 30	0.005
E	50 : 35 : 15	0.006

Table 6 Number of live cells and dead cells on days 1 and 5

Sample	Composition (HA/PCL/GEL)	Day 1		Day 5	
		Live	Dead	Live	Dead
A	50 : 40 : 10	168	39	1191	4
B	50 : 35 : 15	153	9	438	6
C	50 : 30 : 20	119	87	291	4
D	50 : 20 : 30	117	18	137	9
E	50 : 25 : 25	113	30	658	5

Result of osteoblast cell attachment

The attachment of cells on the scaffold was meticulously observed using Scanning Electron Microscopy (SEM) at magnifications of 1000×, 5000×, 10 000×, and 20 000×. Fig. 12 depicts the results of the cell attachment test. Following a 5 days culture period, osteoblast cells adhered successfully to all nanofiber scaffold surfaces, as shown in this image. On the scaffold surface, the ATCC 7F2 osteoblast cells displayed a spreading morphology. Such spreading morphology indicates focal contact with the underlying surface, indicating effective biomaterial adhesion.²⁶ These cell attachment findings are consistent with the cell proliferation test results, which revealed an increase in cell viability from day 1 to day 5 Fig. 12.

An effective scaffold should promote vigorous cell proliferation. The results of this study showed an increase in both cell viability and cell numbers on days 3 and 5, as measured by the percentage of cell viability in the MTT assay and the cell count in the fluorescence microscope. This observed pattern suggests that the scaffold promotes cell proliferation effectively. The nanofiber scaffold's advantageous structure, which includes a large surface area and a porous framework, promotes cellular processes such as adhesion, proliferation, migration, and differentiation. The nanofiber scaffold has outstanding properties such as a large surface area, high porosity, and spatial

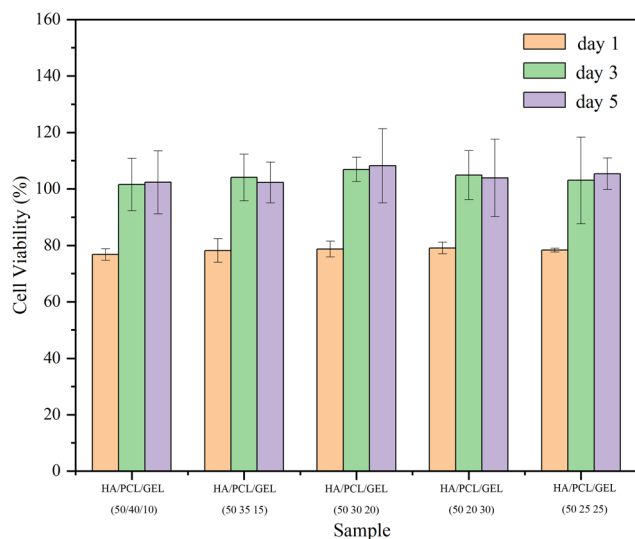


Fig. 8 Graph of cell viability percentage of HA/PCL/gelatin nanofiber scaffold samples (in wt%): (A) 50 : 40 : 10, (B) 50 : 30 : 20, (C) 50 : 25 : 25, (D) 50 : 20 : 30 and (E) 50 : 35 : 15.



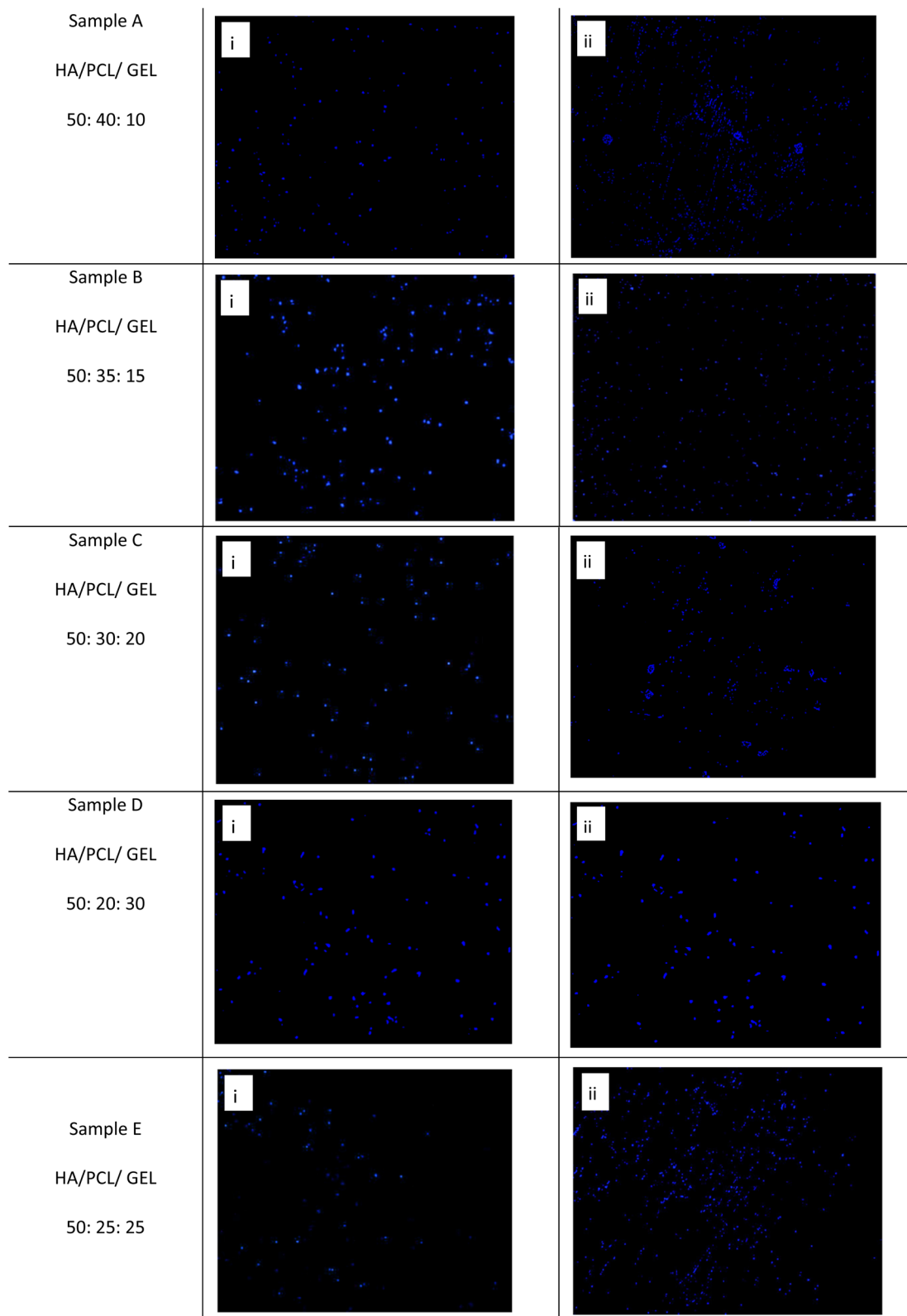


Fig. 9 Live cell visualization of HA/PCL/gelatin nanofiber scaffold samples (in wt%): (A) 50 : 40 : 10, (B) 50 : 30 : 20, (C) 50 : 25 : 25, (D) 50 : 20 : 30 and (E) 50 : 35 : 15. (i) Day 1 and (ii) day 5.

interconnectivity, making it well-suited for efficient nutrient transport, cellular communication, and eliciting cellular responses.²⁷ Higher porosity has been shown to support greater

cell density, resulting in increased cell proliferation. Furthermore, higher porosity scaffolds exhibit higher permeability and cell infiltration.²⁸

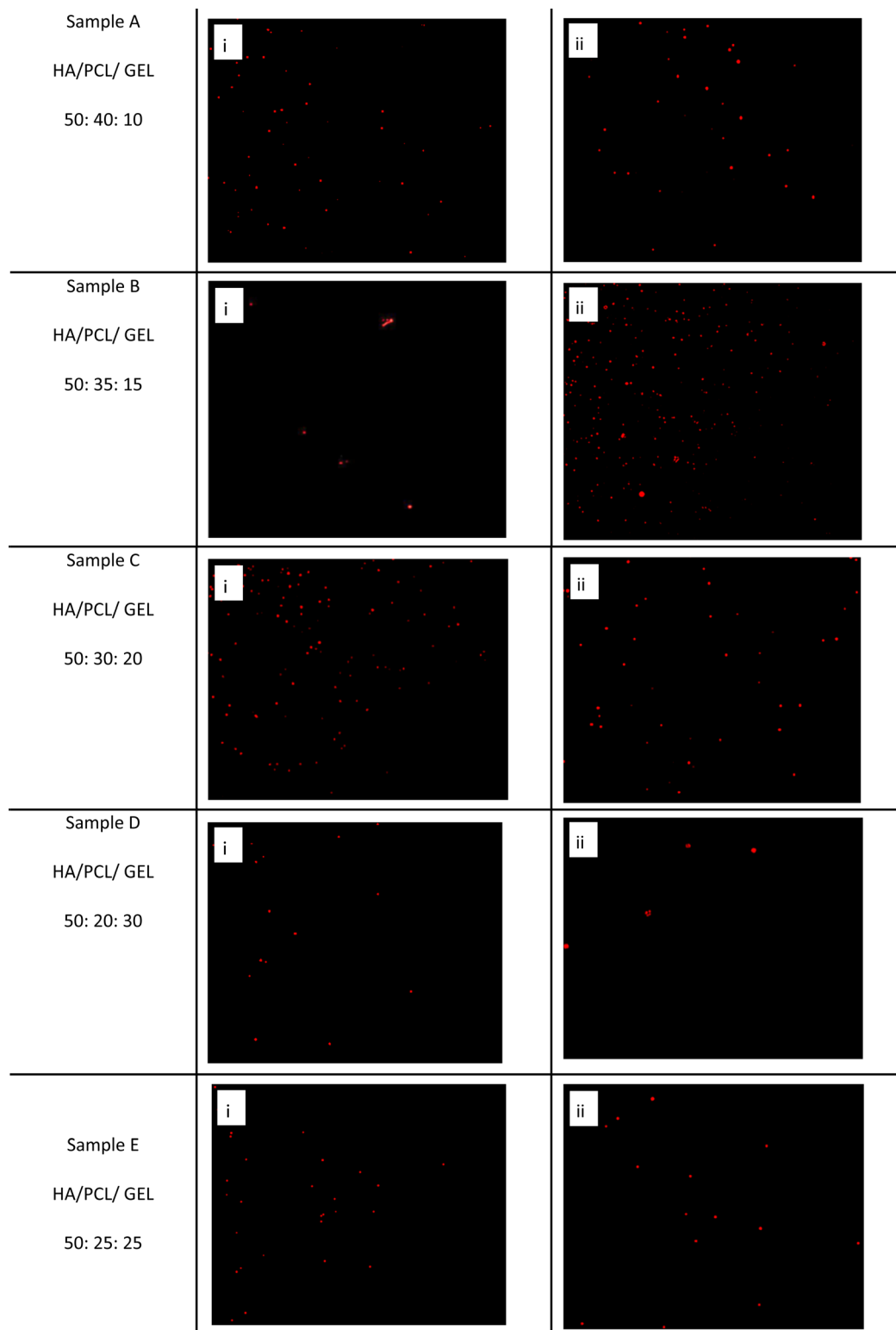


Fig. 10 Visualization of dead cells, HA/PCL/gelatin nanofiber scaffold samples (in wt%): (A) 50 : 40 : 10, (B) 50 : 30 : 20, (C) 50 : 25 : 25, (D) 50 : 20 : 30 and (E) 50 : 35 : 15. (i) Day 1 and (ii) day 5.

Cell attachment is the first stage in cell–scaffold interactions, and it has a significant impact on the cell's ability to proliferate and replicate. On day 5, cell morphology on the scaffold was examined using scanning electron microscopy (SEM) to assess

cell attachment. SEM results show that cell attachment is consistent across all samples, with cells distributed evenly across the scaffolds. Cell attachment is influenced by a variety of factors, the most important of which is pore size. The size of the



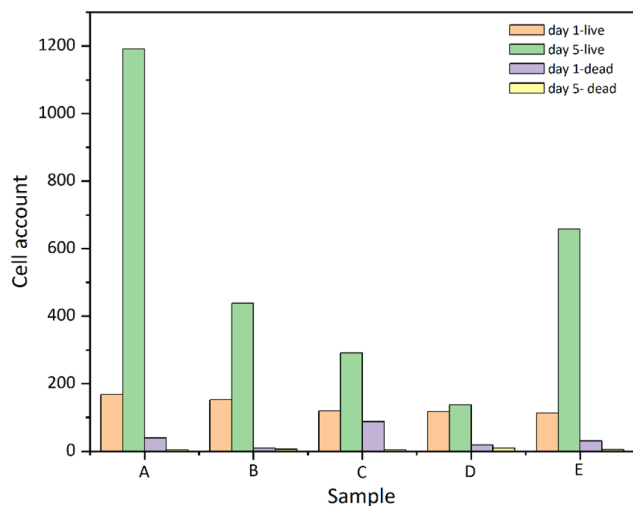


Fig. 11 Number of live cells and dead cells, HA/PCL/gelatin nanofiber scaffold samples (in wt%): (A) 50 : 40 : 10, (B) 50 : 30 : 20, (C) 50 : 25 : 25, (D) 50 : 20 : 30 and (E) 50 : 35 : 15.

pores in biological scaffolds can influence key criteria such as cell attachment, infiltration, and vascularization. Scaffolds with smaller pore sizes have a larger surface area, creating a larger region for cellular attachment.²⁹

Hydroxyapatite, polycaprolactone, and gelatin were found to improve mesenchymal stem cell (MSC) adhesion. Hydroxyapatite, a major component of mammalian hard tissues such as bones and teeth, contributes to polymer/composites' osteoconductivity and bioactivity. The addition of hydroxyapatite not only imparts osteoconductive and bioactive properties, but it also promotes osteoblast proliferation.³⁰ Concurrently, collagen has been shown to promote bone cell proliferation by increasing cell adhesion and enhancing osteogenic cell differentiation.²⁶

In conclusion, the comprehensive tests performed, which entailed the MTT Assay, fluorescence microscopy test, and SEM test, suggest a cohesive framework in the *in vitro* examination of cell interactions on HA/PCL/gelatin nanofiber scaffolds as prospective bone scaffolds. Cell interactions on HA/PCL/gelatin nanofiber scaffolds are effectively demonstrated *in vitro*,

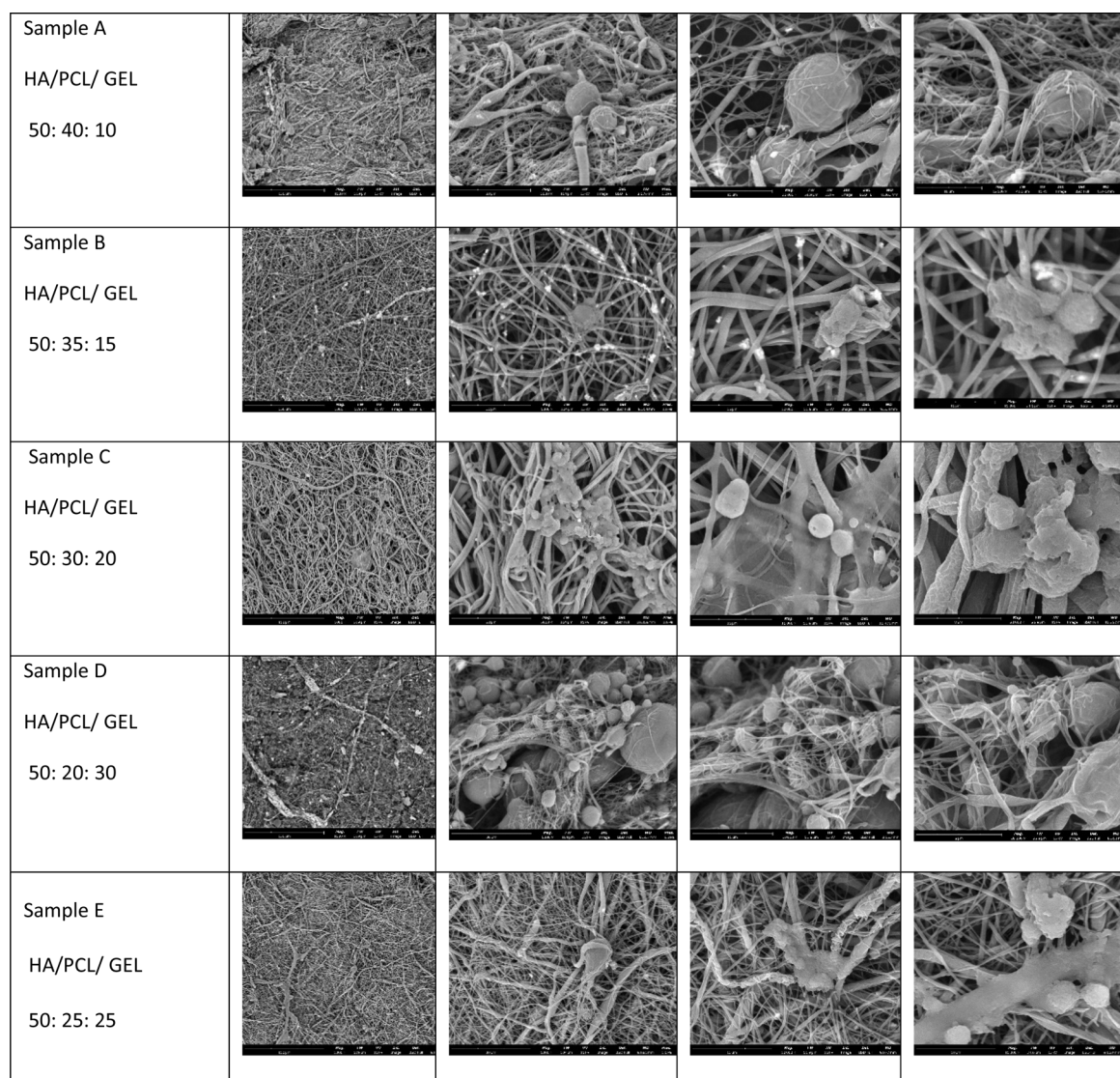


Fig. 12 Cell attachment in SEM test results, HA/PCL/gelatin nanofiber scaffold samples (in wt%): (A) 50 : 40 : 10, (B) 50 : 30 : 20, (C) 50 : 25 : 25, (D) 50 : 20 : 30 and (E) 50 : 35 : 15. From left to right magnification 1000 \times , 5000 \times , 10 000 \times and 200 000 \times .



supporting cell viability, attachment, proliferation, and differentiation. These interactions are critical in promoting the formation of new bone tissue, rendering HA/PCL/gelatin nanofiber scaffolds promising candidates for treating bone defects.

Conclusion

Following extensive investigations, evaluations, and careful considerations, this work validates that HA/PCL/gelatin composites were successfully utilised to fabricate nanofiber scaffolds. The following compositions (represented as HA/PCL/gelatin (in wt%)) were analysed using a variety of criteria: (A) 50 : 40 : 10, (B) 50 : 30 : 20, (C) 50 : 25 : 25, (D) 50 : 20 : 30, and (E) 50 : 35 : 15. All five samples had an identical functional group composition, according to FTIR tests. The SEM test demonstrated that larger fibre diameters, with an average value of 929 ± 175 nm and a range of 369–1403 nm, are correlated with higher PCL concentrations. Interestingly, the maximum porosity percentage discovered was $(77.27 \pm 11.57)\%$, which is thought to be ideal for promoting cell adhesion and growth.

Degradation assessments indicated that all five HA/PCL/gelatin samples degrade at a rate conducive to osteoblast cell proliferation, lasting up to 3.5 months. Tensile strength tests showed that the addition of PCL composition significantly improves tensile strength, reaching a maximum of 1.93 MPa. The interaction between HA/PCL/gelatin nanofiber scaffolds and osteoblast cells was observed to be successful, as evidenced by increased cell viability percentages on days 1, 3, and 5. Furthermore, the fluorescence microscopy test revealed an increased number of live cells (coloured blue) compared to dead cells (coloured red), especially on days 1 and 5. The SEM test confirmed the biocompatibility of the HA/PCL/gelatin nanofiber scaffolds, as evidenced by osteoblast cell attachment and distribution over a five-day seeding period.

Data availability

The data that support the findings of this study are available from the corresponding author upon reasonable request.

Author contributions

Aminatun, Yusril Yusuf, Yessie Widia Sari, Gunawarman: conceptualization, designed the experiments, performed the experiments and collected data, validation, writing and original draft preparation. Aisyah Sujak MK: designed the experiments and review. Djony Izak R., Sofijan Hadi: investigation, review, and editing. Che Azurahaman Che Abdullah: conceptualization, validation, and supervision. Nilam Cahyati, Aminatun, Yusril Yusuf: conceptualization, validation, supervision, review and editing, funding acquisition, and project administration.

Conflicts of interest

The authors declare that they have no known competing financial interests or personal relationships that could influence the work in this article.

Acknowledgements

The authors also would like to acknowledge the use of facilities and technical assistance from the Biomedical Technology and Material Physics Laboratories, Faculty of Science and Technology, Universitas Airlangga. The authors are immensely grateful for the Riset Kolaborasi Indonesia (RKI) Program provided by the Ministry of Education and Culture, the Republic of Indonesia, for financially supporting this research.

References

- 1 B. Dhandayuthapani, Y. Yoshida, T. Maekawa and D. S. Kumar, Polymeric scaffolds in tissue engineering application: A review, *Int. J. Polym. Sci.*, 2011, **2011**, 290602.
- 2 N. Udomluck, H. Lee, S. Hong, S. H. Lee and H. Park, Surface functionalization of dual growth factor on hydroxyapatite-coated nanofibers for bone tissue engineering, *Appl. Surf. Sci.*, 2020, **520**, 146311.
- 3 V. J. Mawuntu and Y. Yusuf, Porous-structure engineering of hydroxyapatite-based scaffold synthesized from Pomacea canaliculata shell by using polyethylene oxide as polymeric porogen, *IOP Conf. Ser.: Mater. Sci. Eng.*, 2018, **432**, 012045.
- 4 W. J. Li, C. T. Laurencin, E. J. Caterson, R. S. Tuan and F. K. Ko, Electrospun Nanofibrous Structure: A Novel Scaffold for Tissue Engineering, *J. Biomed. Mater. Res.*, 2002, **60**(4), 613–621.
- 5 N. Udomluck, W. G. Koh, D. J. Lim and H. Park, Recent developments in nanofiber fabrication and modification for bone tissue engineering, *Int. J. Mol. Sci.*, 2020, **21**, 99.
- 6 H. Liu, X. Ding, G. Zhou, P. Li, X. Wei and Y. Fan, Electrospinning of nanofibers for tissue engineering applications, *J. Nanomater.*, 2013, **2013**, 495708.
- 7 R. Anggraini, M. Sari, T. Suciati, K. Dahlan and Y. Yusuf, Nanostructure of carbonated hydroxyapatite precipitation extracted from pearl shells (*Pinctada maxima*) by pH treatment, *Digest J. Nanomater. Biostruct.*, 2021, **16**(4), 1619–1625.
- 8 M. A. Woodruff and D. W. Hutmacher, The return of a forgotten polymer – Polycaprolactone in the 21st century, *Prog. Polym. Sci.*, 2010, **35**, 1217–1256.
- 9 S. T. Aminatun, Y. W. Sari, M. Sari, K. A. Alamsyah, W. Purnamasari, *et al.*, Biopolymer-based polycaprolactone-hydroxyapatite scaffolds for bone tissue engineering, *Int. J. Polym. Mater. Polym. Biomater.*, 2023, **72**(5), 376–385.
- 10 A. C. Gurlek, B. Sevinc, E. Bayrak and C. Eriskin, Synthesis and characterization of polycaprolactone for anterior cruciate ligament regeneration, *Mater. Sci. Eng., C*, 2017, **71**, 820–826.
- 11 M. Dressler, F. Dombrowski, U. Simon, J. Börnstein, V. D. Hodoroba, M. Feigl, *et al.*, Influence of gelatin coatings on compressive strength of porous hydroxyapatite ceramics, *J. Eur. Ceram. Soc.*, 2011, **31**(4), 523–529.
- 12 P. Chen, L. Liu, J. Pan, J. Mei, C. Li and Y. Zheng, Biomimetic composite scaffold of hydroxyapatite/gelatin–chitosan core-shell nanofibers for bone tissue engineering, *Mater. Sci. Eng., C*, 2019, **97**, 325–335.



- 13 R. Yao, J. He, G. Meng, B. Jiang and F. Wu, Electrospun PCL/Gelatin composite fibrous scaffolds: Mechanical properties and cellular responses, *J. Biomater. Sci., Polym. Ed.*, 2016, **27**(9), 824–838.
- 14 M. R. Qadir, J. Hossan, M. M. Karim, M. J. Hossan, M. A. Gafur and M. R. Kadir, Preparation and Characterization of Gelatin-Hydroxyapatite Composite for Bone Tissue Engineering, *Int. J. Eng. Technol. Sci.*, 2014, **14**(01), 24.
- 15 N. Alharbi, A. Daraei, H. Lee and M. Guthold, The effect of molecular weight and fiber diameter on the mechanical properties of single, electrospun PCL nanofibers, *Mater. Today Commun.*, 2023, **35**, 105773.
- 16 A. Haider, S. Haider and I. K. Kang, A comprehensive review summarizing the effect of electrospinning parameters and potential applications of nanofibers in biomedical and biotechnology, *Arabian J. Chem.*, 2018, **11**, 1165–1188.
- 17 F. H. Zulkifli, F. S. Jahir Hussain, M. S. B. Abdull Rasad and M. Mohd Yusoff, In vitro degradation study of novel HEC/PVA/collagen nanofibrous scaffold for skin tissue engineering applications, *Polym. Degrad. Stab.*, 2014, **110**, 473–481.
- 18 H. A. Permatasari and Y. Yusuf, Characteristics of Carbonated Hydroxyapatite Based on Abalone Mussel Shells (*Halioitis asinina*) Synthesized by Precipitation Method with Aging Time Variations, *IOP Conf. Ser.: Mater. Sci. Eng.*, 2019, **546**, 042031.
- 19 Y. Yusril, P. H. A. Almukarrama, I. K. Januariyasa, M. F. Muarif, R. M. Anggraini, *et al.*, *Karbonat Hidroksiapatit Dari Bahan Alam*, ed. Moulidvi, Gadjah Mada University Press, 2021.
- 20 K. Ramachandran and P. I. Gouma, Electrospinning for Bone Tissue Engineering, *Recent Pat. Nanotechnol.*, 2008, **2**, 1–7.
- 21 K. Phillipson, J. N. Hay and M. J. Jenkins, Thermal analysis FTIR spectroscopy of poly(ϵ -caprolactone), *Thermochim. Acta*, 2014, **595**, 74–82.
- 22 W. B. Hillig, Y. Choi, S. Murtha, N. Natravali and P. Ajayan, An open-pored gelatin/hydroxyapatite composite as a potential bone substitute, *J. Mater. Sci.: Mater. Med.*, 2008, **19**(1), 11–17.
- 23 Q. Zhang, S. Lv, J. Lu, S. Jiang and L. Lin, Characterization of polycaprolactone/collagen fibrous scaffolds by electrospinning and their bioactivity, *Int. J. Biol. Macromol.*, 2015, **76**, 94–101.
- 24 W. Wattanutchariya and W. Changkowchai, Characterization of Porous Scaffold from Chitosan-Gelatin/Hydroxyapatite for Bone Grafting, *Proceedings of the International MultiConference of Engineers and Computer Scientists*, IMECS, Hong Kong, 2014, vol. 2.
- 25 W. Fu, Z. Liu, B. Feng, R. Hu, X. He, H. Wang, *et al.*, Electrospun gelatin/PCL and collagen/PLCL scaffolds for vascular tissue engineering, *Int. J. Nanomed.*, 2014, **9**(1), 2335–2344.
- 26 A. Shams, E. Masaeli and H. Ghomi, Biomimetic surface modification of Three-dimensional printed polylactic acid scaffolds with custom mechanical properties for bone reconstruction, *J. Biomater. Appl.*, 2023, **37**(6), 1042–1053.
- 27 X. Wang, B. Ding and B. Li, Biomimetic electrospun nanofibrous structures for tissue engineering, *Mater. Today*, 2013, **16**, 229–241.
- 28 Á. Paim, I. C. Tessaro, N. S. M. Cardozo and P. Pranke, Mesenchymal stem cell cultivation in electrospun scaffolds: mechanistic modeling for tissue engineering, *J. Biol. Phys.*, 2018, **44**, 245–271.
- 29 C. M. Murphy, M. G. Haugh and F. J. O'Brien, The effect of mean pore size on cell attachment, proliferation and migration in collagen-glycosaminoglycan scaffolds for bone tissue engineering, *Biomaterials*, 2010, **31**(3), 461–466.
- 30 B. Banimohamad-Shotorbani, A. Rahmani Del Bakhshayesh, A. Mehdipour, S. Jarolmasjed and H. Shafaei, The efficiency of PCL/HAp electrospun nanofibers in bone regeneration: a review, *J. Med. Eng. Technol.*, 2021, **45**, 511–531.

